Supplementary Information : Understanding the Impact of Ammonium Ion Substitions on Heterogeneous Ice Nucleation

Katarina E. Blow[a], Thomas F. Whale[b], David Quigley[a] and Gabriele C. Sosso[b]
[a]*Department of Physics, University of Warwick, Gibbet Hill Road, Coventry CV4 7AL, United Kingdom*
[b]*Department of Chemistry, University of Warwick, Gibbet Hill Road, Coventry CV4 7AL, United Kingdom*

Here, we provide supplementary information about:

- A schematic representation of the steps involved in Rick's algorithm[1] (Figure S1)
- The stopping criteria we have used to determine the number of possible structures relative to the substitution of an ammonium ion into the ice lattice (Figure S2)
- The comparison between the energy of selected structures – with or without the presence of the ammonium ion – according to the TIP4P/Ice and CHARMM36 force fields (see main text) and electronic structure calculations (Figure S3)
- The stopping criterion in terms of the maximum force acting on any atom in the context of the energy minimisations conducted via GROMACS to calculate the energy of ice structures – with or without the presence of the ammonium ion. (Figure S4)
- A comparison of the number of configurations per set on the observed spread of computed minimum energies (Figure S5)
- Minimum energy spreads for ammonium-containing ice at seven and eight connections to a base with a total charge of 1.20 e (Figure S6)
- A comparison of median energies across all possible number of connections for pure ice, at a number of different surface charges (Figure S7)

S1 Electronic structure calculations

In order to to verify that the combination of the CHARMM36 force field and the TIP4P/Ice model of water would yield accurate results in terms of the energy of the structures we are interested in, we have compared – for a small selection of said structures – our results with the outcomes of electronic structure calculations. In particular, we have performed density functional theory (DFT) calculations using the mixed Gaussian and Plane-Waves (GPW) method implemented in the CP2K package[2]. We have used two different exchange-correlation (XC) functionals, namely the widely used PBE[3] and the fully self-consistent, non-local vdW-DF[4] XC functional, to assess the reliability of our results. Goedecker-type pseudopotentials[5] have been employed. The Kohn-Sham orbitals were expanded in a Double-Zeta Valence plus Polarisation (DZVP) Gaussian-type basis set, while the plane wave cutoff for the finest level of the multi-grid REF has been set to 400 Ry to efficiently solve the Poisson equation within periodic boundary conditions using the Quickstep scheme[2]. Brillouin zone integration was restricted to the supercell Γ-point. A dipole correction[6] has been applied to the electrostatic potential to compensate for the surface dipole. These settings ensure an accuracy of the resulting total energy of 6 meV/atom.

The results are summarised in Figure S3. We obtain a very good agreement between TIP4P/Ice results and DFT results in the case of ice (without the presence of the ammonium ion) – panel (a) of Fig. S3. We also note that the PBE and vdW-DF XC functionals yield practically identical results. As such, we have restricted the analysis of the structures containing the ammonium ion (panel (b) of Figure S3) to the PBE XC functional alone. In this case, the agreement between the TIP4/Ice + CHARMM36 combination and DFT is not optimal. Crucially, however, we remark that the energy differences involved in the discrepancies between the two sets of results are very small – i.e. within the uncertainty associated with our DFT calculations (6 meV/atom, see above).

Notes and references

1 S. W. Rick and A. Haymet, *The Journal of chemical physics*, 2003, **118**, 9291–9296.
2 J. VandeVondele, M. Krack, F. Mohamed, M. Parrinello, T. Chassaing and J. Hutter, *Computer Physics Communications*, 2005, **167**, 103–128.
3 J. P. Perdew, K. Burke and M. Ernzerhof, *Phys. Rev. Lett.*, 1996, **77**, 3865–3868.
4 M. Dion, H. Rydberg, E. Schröder, D. C. Langreth and B. I. Lundqvist, *Phys. Rev. Lett.*, 2004, **92**, 246401.
5 S. Goedecker, M. Teter and J. Hutter, *Phys. Rev. B*, 1996, **54**, 1703–1710.
6 L. Bengtsson, *Phys. Rev. B*, 1999, **59**, 12301–12304.

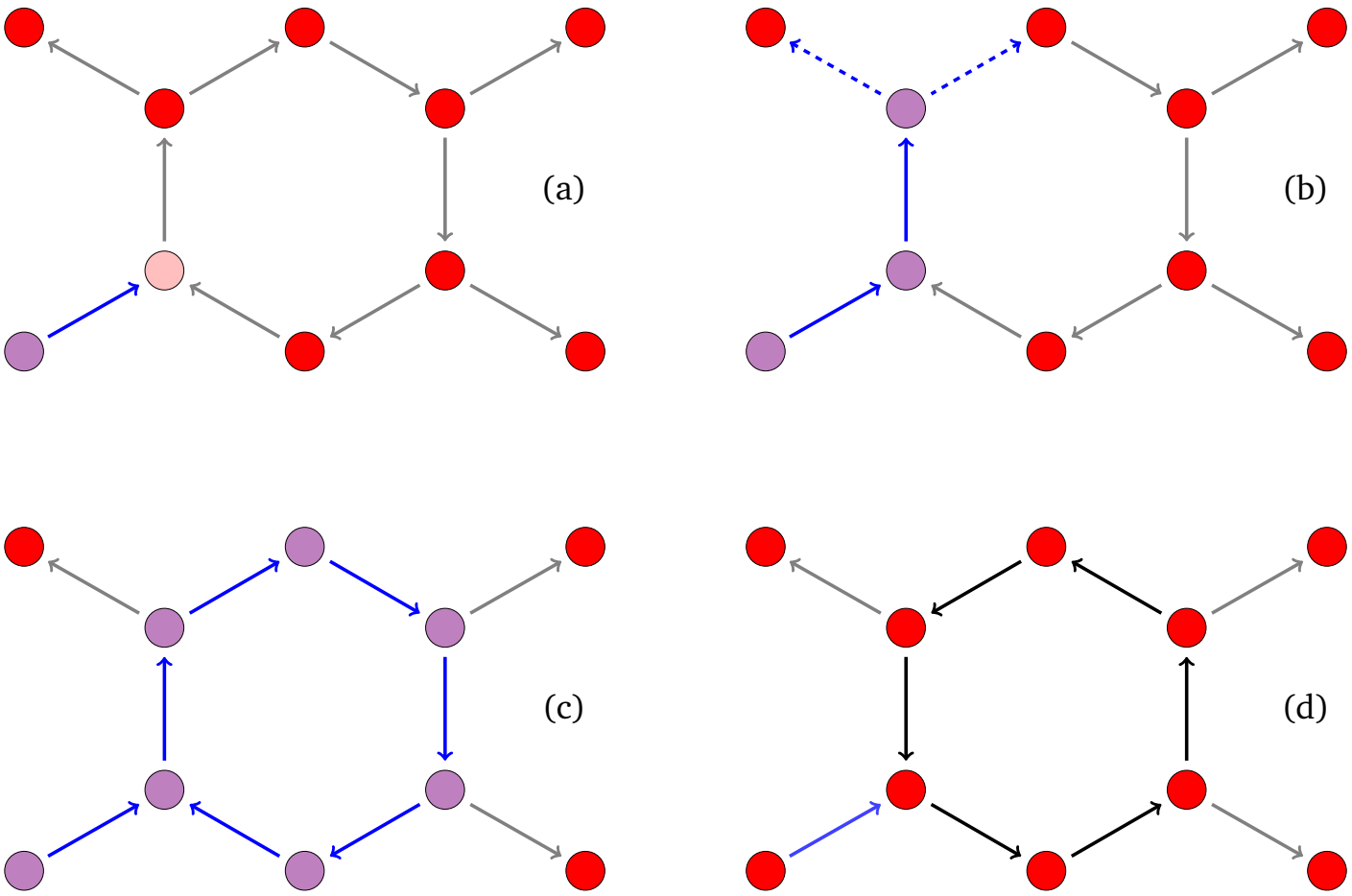

Fig. S1 Schematic representation of Rick's algorithm. The red circles represent oxygen atoms (vertices in the graph representation), and the grey lines represent donated/accepted hydrogen bonds (in the graph representation, these are the edges of the directed graph). Only intra-bilayer hydrogen bonds are shown, inter-bilayer bonds are such that all oxygen atoms have two donated and two accepted hydrogen bonds. (a) In the first step of Rick's algorithm, an oxygen atom (highlighted purple) and bond (highlighted blue) are chosen at random from all possible atoms/bonds. Here, we are following a path of donated hydrogen bonds from chosen nodes, with the next node in the path decided by the chosen bond (highlighted pink). (b) At each subsequent node along the path, there is a random choice of donated hydrogen bond to be made – for the purple atom at the end of this path, these are highlighted as blue dashed lines to distinguish from the solid blue path. The inter-bilayer bond (not shown) is *not* a possible continuation of the path, as it is an accepted hydrogen bond. (c) The path is terminated when it has formed a complete loop. It is not necessary for all of the path to be within the loop, only for a loop to have formed at some point within the path. (d) Finally, all of the bonds within the loop (highlighted black) change direction. This does not lead to any violation of the number of donated/accepted hydrogen bonds. Note that the initial edge (still highlighted blue) was outwith the formed loop, and therefore this bond has not changed direction. This is now a new structure, and the procedure can begin again with a new random choice of atom and bond.

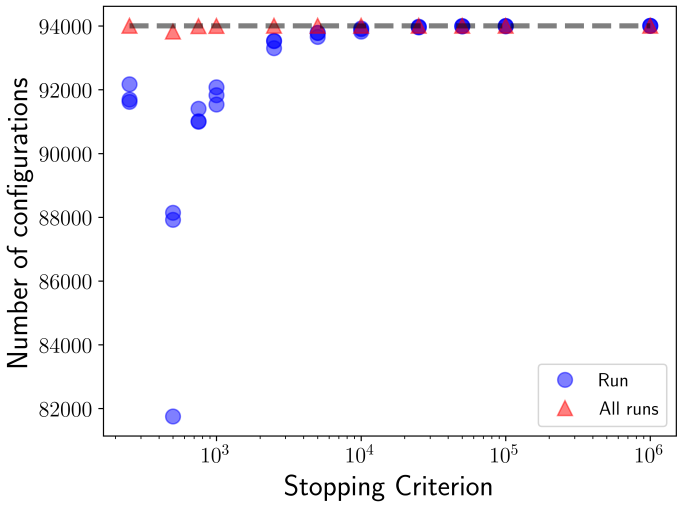

Fig. S2 Comparison of different stopping criteria for ice containing an ammonium in the contact layer with all possible connections fixed to the base. The blue circles represent the number of structures found from a single run at a stopping criterion, and the red triangles show the total number of structures found from a comparison of the three runs represented by blue circles. The grey line shows the total number of structures found from all runs. Differences arise from the stochastic nature of the starting configurations and Rick's algorithm. The outlier at ≈8,200 structures indicates a poor combination of these parameters, although this large difference in absolute structures only corresponds to a small difference in entropy ($\approx 1\%$).

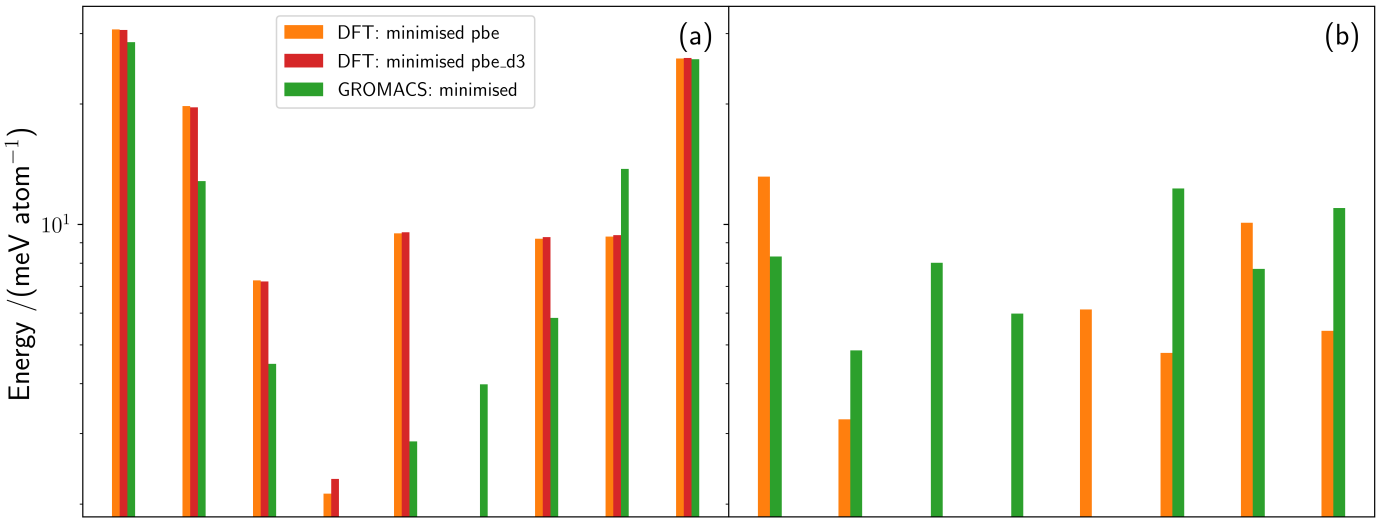

Fig. S3 Comparison of the minimised energy of a pure ice structure in GROMACS with comparable minimised energies from density functional theory (DFT), with energies shifted such that the minimum energy configuration (as determined by each procedure) is 0. The maximum variation between the GROMACS and DFT results are within the expected accuracy of DFT. Panel (a) shows the energies of pure ice, with a variety of connections to the base, whereas panel (b) shows the energies of ammonium-containing ice, where the ammonium is in various layers and there are a variety of connections to the base.

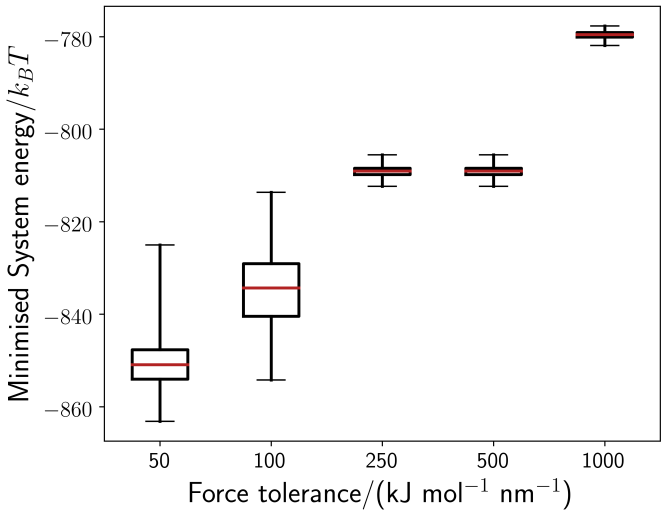

Fig. S4 Comparison of the minimised energy of a pure ice structure with all possible fixed connections to the base, for different force tolerances in GROMACS. The whiskers show the extent of the energy range, with the box representing the first and third quartiles, and the red line showing the median. A force tolerance of 50 kJ mol^{-1} nm^{-1} led to $\approx 15\%$ of the structures being mechanically unstable (removed for this plot), whereas no mechanical instability was observed for the other force tolerances. 100 kJ mol^{-1} nm^{-1} was chosen as it led to significant minimisation without substantial fractions of mechanically unstable structures.

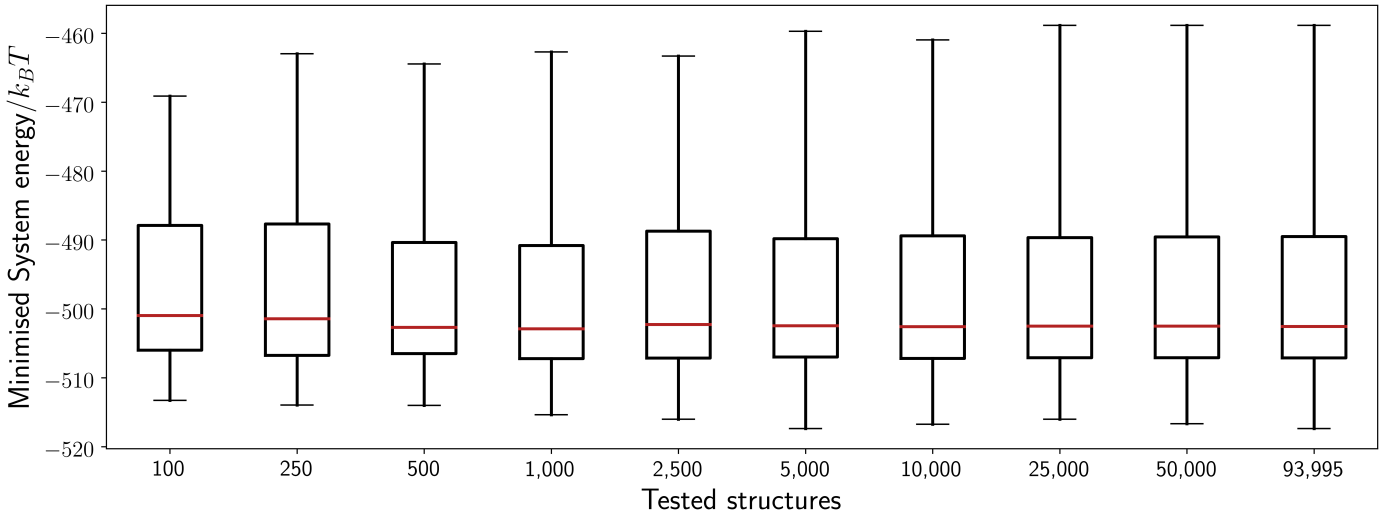

Fig. S5 Comparison of the computed minimised energies of different sizes of sets (containing different numbers of hydrogen bond configurations of a possible 93,995) for ice containing an ammonium in the contact layer with all possible connections fixed to the base. The whiskers show the extent of the energy range, with the box representing the first and third quartiles, and the red line showing the median. Any mechanically unstable structures have been removed.

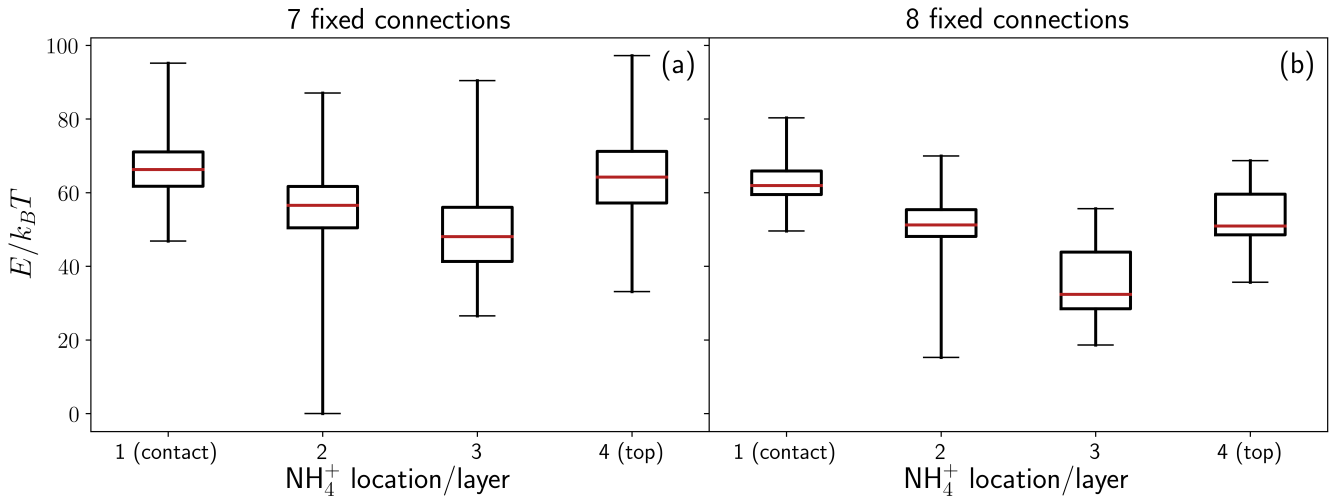

Fig. S6 Minimised energies of ammonium-containing ice for sets of configurations with (a) seven and (b) eight (of a possible eight) fixed connections to the base, which has a charge of 1.20 e across the footprint of the ice. The whiskers show the extent of the energy range, with the box representing the first and third quartiles, and the red line showing the median. The energies have been shifted so that the minimum energy of all plotted configurations is 0. Any mechanically unstable structures have been removed.

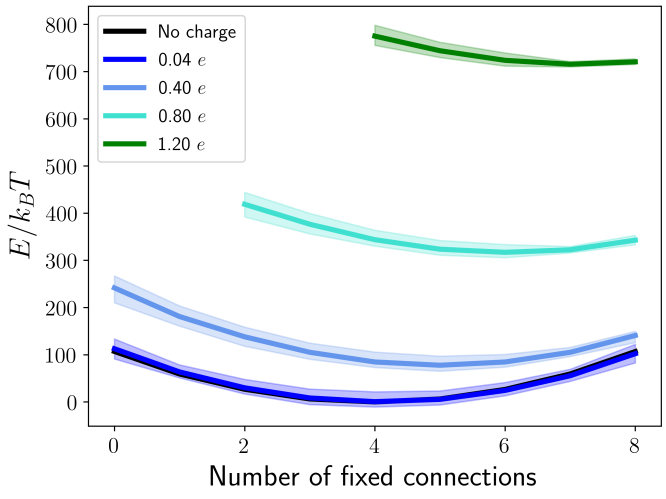

Fig. S7 Minimised energies of pure ice for different surface charges. Charges (in the legend) give the total charge across the footprint of the original ice cell, shifted such that the minimum energy over all configurations is 0. The lines give the median energy of the set of structures, with the shaded areas representing the minimum/maximum energy configuration where the energy is within three standard deviations of the median energy of the set. The no charge line lies under the 0.04 e charge line and is therefore minimally visible. Any mechanically unstable structures have been removed – where there were a significant number of these, no energy is shown.